

IR IMAGE, COURTESY DR. JOHN KEYSERLINGK

# Thermal Image Analysis for Polygraph Testing

## *Two-Dimensional Physiological Measurements Can Serve As an Additional Scoring Channel for Increased Accuracy*

**P**olygraph testing is a standard security procedure favored by the U.S. government. The objective of polygraph testing is to ascertain if the subject under investigation truthfully or deceitfully answers the questions at hand. Specially trained psychologists structure the questions to maximize elicitation. During the testing three physiological parameters are monitored closely:

- a) blood volume and pulse changes
- b) respiratory changes
- c) electrodermal activity.

They are all recorded using invasive methods and produce scalar values over time (signals). Then, a scoring system is used to quantify the subject's response and classify it as deceitful or truthful. An extensive account of state-of-the-art poly-

graph methods and systems can be found in [3].

The success rate for polygraph testing varies, but on average it is in the neighborhood of 90%. The U.S. government is interested in increasing this rate through the use of additional information channels [4]. One very promising channel is the use of infrared facial image analysis. There are several advantages to this method.

1) It is noninvasive. This is very important in the context of polygraph testing where it is crucial for the subject to feel as comfortable as possible.

2) After appropriate processing the thermal imagery can yield physiological information similar to one of the traditional polygraph channels; i.e., blood flow rate. The major difference is that this in-

Ioannis Pavlidis<sup>1</sup> and James Levine<sup>2</sup>

<sup>1</sup>University of Houston

<sup>2</sup>Mayo Clinic

**Table 1. The ten Zone Comparison Test questions used in our polygraph test.**

	Zone Comparison Test	Comment
1	Is your name ____?	Irrelevant: not scored
2	Regarding whether you stabbed that woman today, do you intend to answer my questions truthfully?	Sacrifice relevance: scored
3	Do you understand that I will not ask any trick or surprise questions on this test	Symptomatic: not scored
4	Before arriving at Fort Jackson, did you ever hurt someone who trusted you?	Comparison: scored
5	Did you stab that woman this morning/afternoon?	Relevant: scored
6	Before arriving at Fort Jackson, did you ever lose your temper when you shouldn't have?	Comparison: scored
7	Did you stab that woman downstairs this morning/afternoon?	Relevant: scored
8	Is there a question you are afraid I will ask about even though I said I would not?	Symptomatic: not scored
9	Before this year, did you ever take anything important that didn't belong to you?	Comparison: scored
10	Do you have that stolen \$20 on you right now?	Relevant: scored

formation is now two-dimensional (2-D) and not one-dimensional (1-D) across the time line. This is at least an order of magnitude more information than the traditional channel can generate.

In this article we will describe our experimental design of an infrared facial image analysis system, the image acquisition setup, the method we follow to convert raw thermal data to blood flow rate data, the scheme we use to classify deceptive from nondeceptive subjects, and an analysis of our experimental results. We will also discuss our plan for future research.

### Experimental Design

We have run standard polygraph tests on a number of subjects. The polygraph tests were designed around a mock crime scenario. The crime scene involved the stabbing of a woman with a screwdriver. Some of the subjects were programmed “innocent,” and some were programmed “guilty.” The guilty subjects enacted the crime as if it were real. A mannequin played the role of the stabbed woman in the crime scene. The theft of a \$20 bill has been identified as the motive for the crime. The innocent subjects did not have any knowledge or association with the crime scene. Psychologists in the Department of Defense National Polygraph Institute (DoDPI) structured the type and sequence of questions. There were two sets of questions the subjects had to address: Ten full questions composing the so-called Zone Comparison Test (see Table 1) and six short questions composing the so-called Guilty Knowledge Test (GKT) (see Table 2). In the Zone Comparison Test the subject was required to answer each question with a simple “yes” or “no.” In the GKT test, the subject had to read through a list of potential murder weapons, only one of which was the murder weapon pertaining to the case. His/her physiological response was gauged for each word. In traditional polygraph test-

## In addition to the traditional invasive measurements, we recorded digital clips of thermal video data for each question of each subject.

ing, a strong physiological response is anticipated when a guilty subject hears the murder weapon word.

First, the polygraph examiner runs through the two question sets just to familiarize the subject with the content of the examination. The subject is not required to answer any of the questions at this point and nothing is scored. Then, the examiner repeats the questions and the subject is required to answer this time. This is the first official chart. There are two more charts that follow. In all three charts the Zone Comparison Test questions remain exactly the same. In the GKT questions, however, the position of the murder weapon word changes from run to run. The position of the murder weapon word in the first two runs of our testing is shown in Table 2.

In traditional polygraphy all three charts/runs are scored. By looking into the details of the scoring scheme, however, we notice that three questions in the Zone

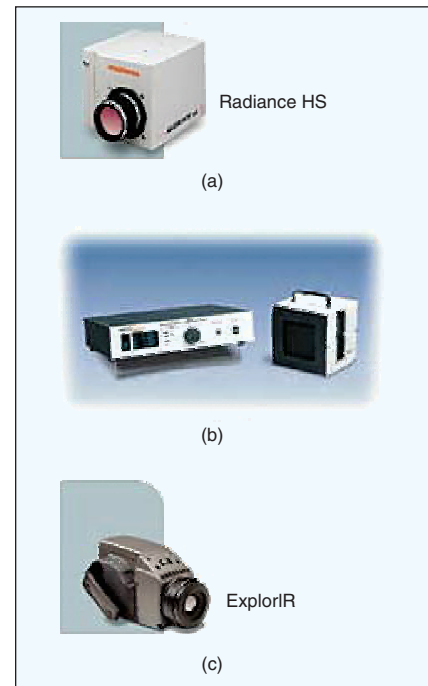
Comparison Test are never scored (see Table 1). These are either irrelevant or symptomatic questions and serve as fillers from the psychological point of view. The rationale for having the subject perform the Zone Comparison and GKT tests three times is to average the contribution of a possible noisy response. Of course, the average intensity of the physiological response is expected to be lower for charts/runs 2 and 3 in comparison to chart/run 1. This is attributable to the repetitive nature of the exercise and is taken into account in the scoring scheme.

In addition to the traditional invasive measurements we recorded digital clips of thermal video data for each question of each subject. Our recording started right before the examiner expressing the question until right after the subject was giving his/her answer. For the Zone Comparison Test questions the average recording length was 300 frames at 30 frames/s. For the GKT questions the average recording length was 150 frames at 30 frames/s.

We have recorded only the first two charts/runs for thermal image processing

**Table 2. The first two runs of the GKT questions for our polygraph test.**

	GKT Questions - Run 1	GKT Questions - Run 2
1	Irrelevant	Irrelevant
2	Irrelevant	Screwdriver (murder weapon)
3	Irrelevant	Irrelevant
4	Irrelevant	Irrelevant
5	Screwdriver (murder weapon)	Irrelevant
6	Irrelevant	Irrelevant



**1. (a) The cooled mid-infrared camera by Raytheon used in the polygraph experiments. (b) The black body and its controller by Santa Barbara Infrared. (c) The uncooled far-infrared camera by Raytheon. We used the uncooled model in the past for lab experiments involving strong startle stimuli, where physiological responses were more acute and thermal sensitivity less important.**

and analysis. This was due to our limited resources. So far, we have analyzed only the first chart.

### Image Acquisition Setup

We have used a cooled mid-infrared camera, the Radiance HS by Raytheon (see Figure 1). The focal plane area (FPA) of the camera is sensitive to the 3-5  $\mu\text{m}$  waveband and its size is  $256 \times 256$  pixels.

We have anticipated that temperature sensitivity will be very important in our experiments since we expected only subtle stimuli within the mock crime context and consequently infinitesimal facial temperature changes. The thermal sensitivity of the Raytheon Radiance HS is  $\text{NEDT} = 0.025 \text{ }^\circ\text{C}$ . By comparison, the thermal sensitivity of the Raytheon ExplorIR we used in previous lab experiments [1], [2]

is about an order of magnitude worse ( $\text{NEDT} = 0.15 \text{ }^\circ\text{C}$ ).

To ensure the highest level of temperature reading accuracy we calibrated the Raytheon Radiance HS camera using an external black body. Specifically, we used the 2008 Model by Santa Barbara Infrared with thermal sensitivity equivalent to that of our camera ( $\text{NEDT} = 0.025 \text{ }^\circ\text{C}$ ). We set the minimum and maximum calibration temperatures to  $T_{\min} = 29 \text{ }^\circ\text{C}$  and  $T_{\max} = 38 \text{ }^\circ\text{C}$ , respectively. Based on our experimental experience these are the temperature extremities one can find across the human face.

Since we operated in the mid-infrared spectrum, to eliminate any effect on the measurements from illumination we performed the experiments in a dimly lit room. The thermal camera was connected

and controlled by a PC that ran special software. Video clips for each question and subject were recorded directly on a CD-RW medium.

### Heat Transfer Modeling

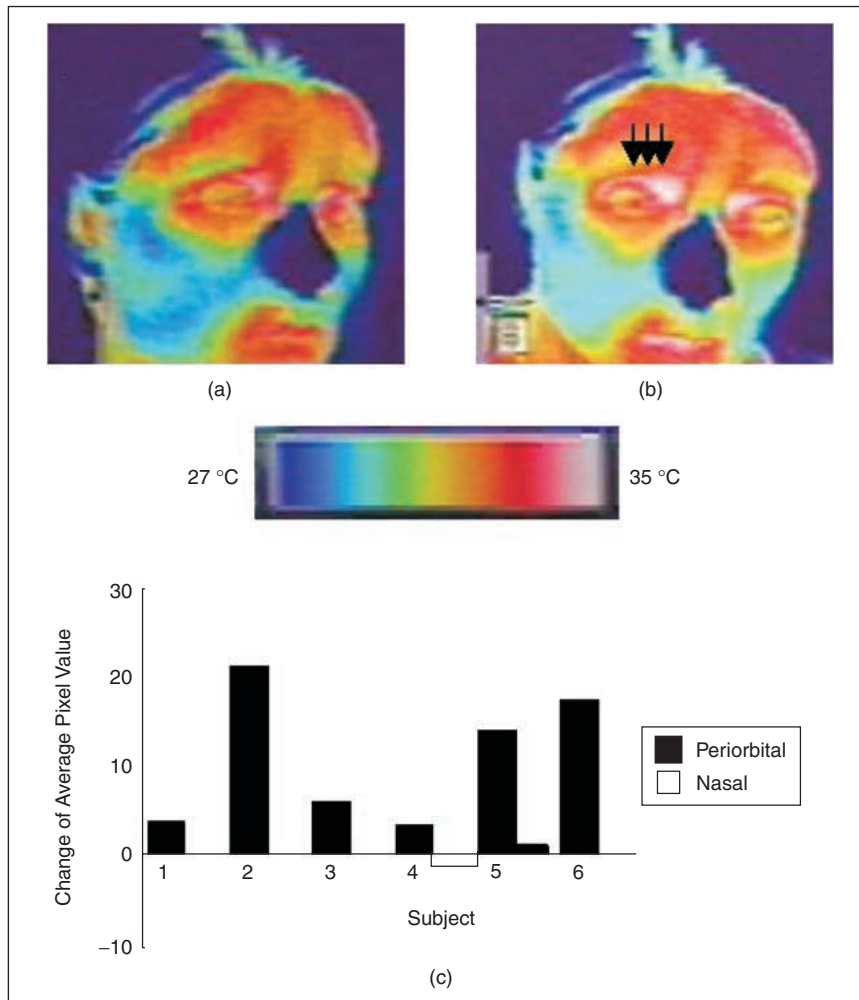
#### Previous Work

In [1] and [2] we described a method for detecting anxiety through thermal facial image analysis. We reproduced anxiety feelings by applying a startle stimulus to subjects. Specifically, we allowed subjects to relax for about 10 min in a dimly lit room. The ambient temperature at the room was set at  $70 \text{ }^\circ\text{F}$  and the subjects fasted for at least two hours before the experiment. Then, without prior notice, we produced an instantaneous loud noise (60 dB) and recorded via a far-infrared camera (ExplorIR by Raytheon) the face of the subject from just before to just after the startle event. The results of thermal image analysis demonstrated that fright is accompanied by significant warming in the periorbital area (see Figure 2). This warming was attributable to increased blood circulation in the area around the eyes. The whole pattern makes physiological and evolutionary sense since it represents (a hitherto unidentified) mechanism to facilitate rapid eye movements during preparedness for flight.

#### From Raw Thermal Data to Blood Flow Rate Data

In the polygraph test setting one could visually observe that the temperature changes around the eyes and in the face generally were very subtle, almost unnoticeable (see Figure 3). This was in stark contrast to the very noticeable temperature changes in the case of the startle experiments (see Figure 2). We argue that this disparity is due to the comparatively subtle stress imposed on the polygraph subjects in the context of the mock crime scenario. Therefore, our goal was to find a method that would amplify the weak pattern buried in the raw thermal data.

The fluctuation of temperature in the various facial areas is primarily due to the changing blood flow rate. Heat transfer modeling shows that the blood flow rate is inversely proportional to the square of the skin temperature deviation from the temperature at the core of the human body. This nonlinear relation amplifies the weak temperature change patterns observed in polygraphy subjects and brings the infor-



**2. Thermal images of the face for a subject (a) before and (b) 300 ms after an instantaneous startle. Arrows indicate local warming in the periorbital area. The color bar depicts the false coloring scheme from the lowest ( $27 \text{ }^\circ\text{C}$ ) to the highest ( $35 \text{ }^\circ\text{C}$ ) temperature. (c) Changes of the average pixel value in the periorbital and nasal areas with auditory startle. The changes are depicted for each subject ( $n = 6$  subjects). Positive deviation represents local warming and negative deviation represents cooling.**

mation noise down to the levels of the startle stimulus experiments (see Figure 3).

Specifically, at thermal equilibrium we model the heat balance equation for human skin tissue as proposed in [5]:

$$Q_r + Q_e + Q_f = Q_c + Q_m + Q_b,$$

where  $Q_r$  = the heat radiated from the subject to the air in units of calories;  $Q_e$  = the basic evaporated heat;  $Q_f$  = the heat loss via convection into the air neighboring the skin surface;  $Q_c$  = the heat conducted by subcutaneous tissue;  $Q_m$  = the heat corresponding to the metabolic rate of cutaneous tissue; and  $Q_b$  = the heat gain/loss via convection attributable to blood flow of subcutaneous blood vessels.

If we observe skin-temperature change ( $\Delta T_s$ ) in a short period ( $\Delta t$ ), the following equation results:

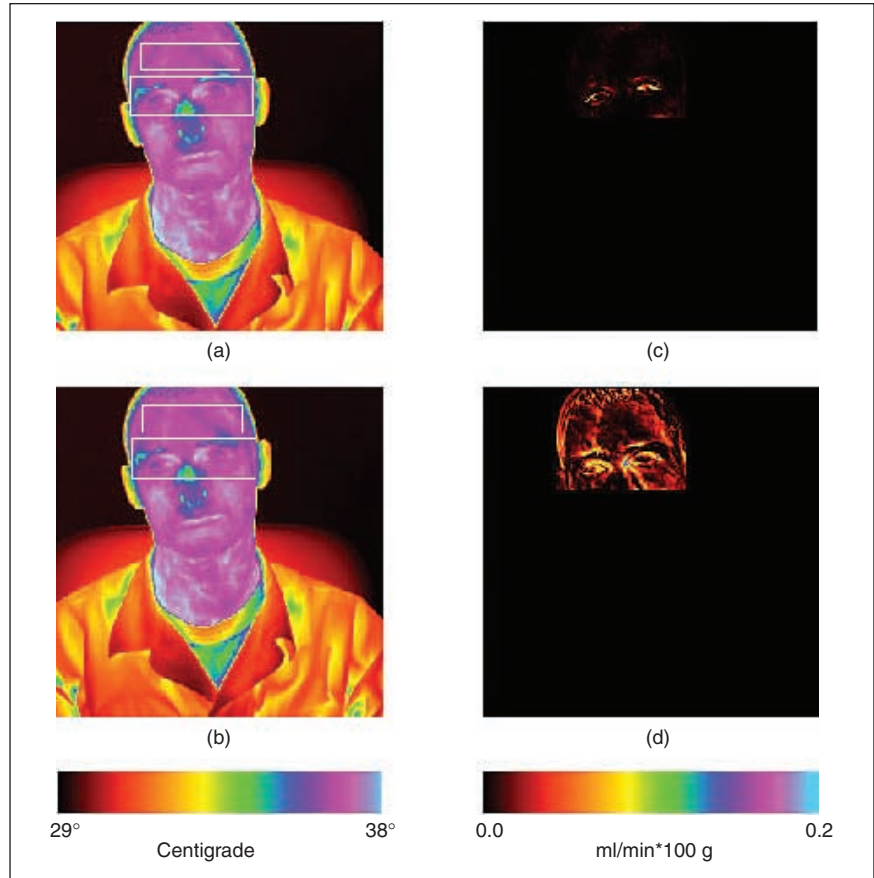
$$C_s \Delta T_s = -(\Delta Q_r + \Delta Q_e + \Delta Q_f) + (\Delta Q_c + \Delta Q_m + \Delta Q_b) \quad (2)$$

where  $C_s$  = the heat capacity of skin.

For short periods of time ( $\Delta t$ ), and assuming that the subject did not have recently a sizeable meal, we can consider the term  $\Delta Q_m$  as negligible. The terms  $\Delta Q_r$ ,  $\Delta Q_e$ , and  $\Delta Q_f$  are shown to be of magnitude approximately 1/100 less than the magnitude of  $\Delta Q_b$  [6]. Therefore,

$$\begin{aligned} C_s \Delta T_s &\approx \Delta Q_c + \Delta Q_b \\ &= \alpha p_c V_{S_2} (T_B - T_{S_2}) S \\ &\quad - \alpha p_c V_{S_1} (T_B - T_{S_1}) S \\ &\quad + K_c (T_B - T_{S_2}) / (3d) \\ &\quad - K_c (T_B - T_{S_1}) / (3d) \\ &= \alpha p_c \Delta V_S T_B S \\ &\quad - \alpha p_c (V_{S_2} T_{S_2} - V_{S_1} T_{S_1}) S \\ &\quad - K_c \Delta T_S / (3d) \\ &= \alpha p_c \Delta V_S T_B S - \alpha p_c (V_{S_1} + \Delta V_S) \\ &\quad \cdot (T_{S_1} + \Delta T_S) - V_{S_1} T_{S_1}) S \\ &\quad - K_c \Delta T_S / (3d) \\ &= \alpha p_c \Delta V_S T_B S - \alpha p_c \Delta V_S T_{S_1} S \\ &\quad - \alpha p_c V_{S_1} \Delta T_S S - \alpha p_c \Delta V_S \Delta T_S S \\ &\quad - K_c \Delta T_S / (3d) \\ &= \alpha p_c \Delta V_S (T_B - T_{S_1}) S \\ &\quad - \alpha p_c V_{S_1} \Delta T_S S \\ &\quad - \alpha p_c \Delta V_S \Delta T_S S - K_c \Delta T_S / (3d) \end{aligned} \quad (3)$$

where  $\alpha = 0.8$  (countercurrent heat exchange in a warm condition);  $p_c = 0.92$  cal/mL/K (heat capacity of blood);  $V_{S_i}; i=1,2$  = the skin blood-flow rate at



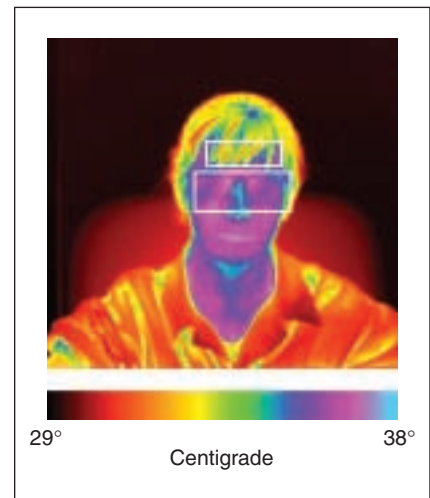
3. (a) Raw thermal image of subject 3 answering Question 10 (toward the beginning). (b) Raw thermal snapshot of subject 3 answering Question 10 (toward the end). The difference between the two left images is imperceptible. The rectangles delineate the periorbital and forehead areas under monitoring. (c) Visualization of the blood flow rate in subject's 3 face as he answers Question 10 (toward the beginning). (d) Visualization of the blood flow rate in subject 3's face as he answers Question 10 (toward the end). The difference between the two right images is significant. The color bars index the range of the temperature and blood flow rate intensities from the lowest to the highest value.

times  $t_1$  and  $t_2$ ;  $T_B = 310$  K (blood temperature in the core);  $T_{S_i}; i=1,2$  = the skin temperature at times  $t_1$  and  $t_2$ ;  $S$  = the thickness of the skin;  $K_c = 0.168$  kcal/m/h/K (thermal conductivity of skin); and  $d$  = the depth of core temperature point from skin surface.

After differentiating, we obtain the following equation:

$$\begin{aligned} C_s \frac{dT_S}{dt} &\approx \alpha p_c \frac{dV_S}{dt} \\ &\quad \times (T_B - T_S) S - \alpha p_c V_S \frac{dT_S}{dt} \\ &\quad \times S - \alpha p_c \frac{dV_S}{dt} \frac{dT_S}{dt} S \\ &\quad - K_c \frac{dT_S}{dt} / (3d). \end{aligned} \quad (4)$$

If we ignore the term involving  $(dV_S/dt)(dT_S/dt)$ , we obtain the following equation:



4. A female subject with hair banks obscuring the forehead area. The exact forehead and periorbital areas under monitoring are delineated by the white rectangles.

$$\frac{dV_S}{dt} = \frac{T_B(C_S + K_c / (3d)) - C}{(T_B - T_S)^2} \frac{dT_S}{dt}, \quad (5)$$

where  $C$  is a constant.

For calibrated thermal imagery, we can calculate the discrete-time approximation to the derivative of the tempera-

ture  $dT_S/dt$  as the difference between a pair of images normalized by the number of sample frames between the respective acquisition times. The expression  $T_B(C_S + K_c / (3d)) - C$  represents a constant. Therefore, we can estimate the term  $dV_S/dt$  except for an unknown scale fac-

tor. The expression for  $dV_S/dt$  can be integrated numerically to obtain an estimate for  $V_S$ .

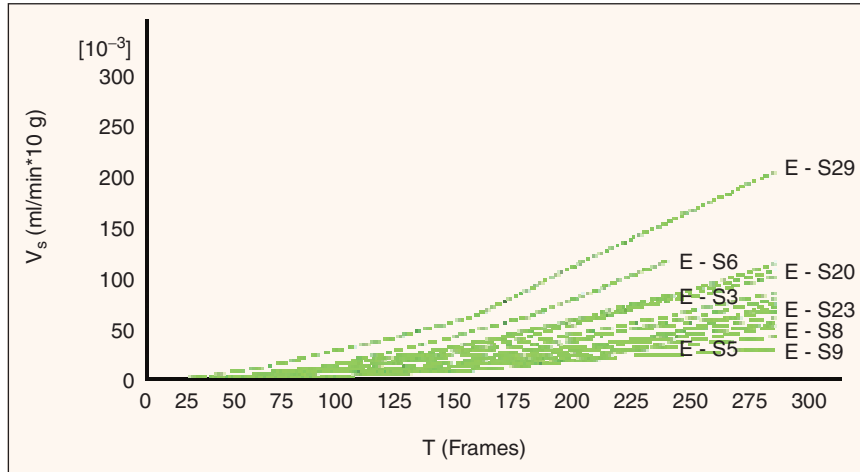
By solving (5) for every pixel in the image we transform the raw thermal data to blood flow rate data. To ensure a meaningful application of (5) we crop the image so that it contains only the subject's face and no background. We perform the cropping at the first frame of each video clip, and the cropping dimensions apply across the time line until the end of the particular question-answer session. This assumes a stationary subject for the short duration (5-10 s) of the question-answer session. Based on our experimental experience the "stationary subject" assumption is realistic. Occasionally, however, some of the more agitated subjects move noticeably even within short time periods. In these cases the heat transfer equation (5) is applied on the wrong points across the time line and its solution should not be considered reliable.

Also, we provide the opportunity for the user to delineate the periorbital and forehead areas for each subject in each question [see Figure 3 (a) and (b)]. The delineation takes place on the first frame of the video clip and is also based on the "stationary subject" assumption. Within the delineated periorbital and forehead areas we compute the respective average blood flow rates for each frame. This produces two signals across the question time line: one "eye" and one "forehead" signal. We use these signals as input to our pattern recognition algorithm for subject classification to the deceptive or nondeceptive category.

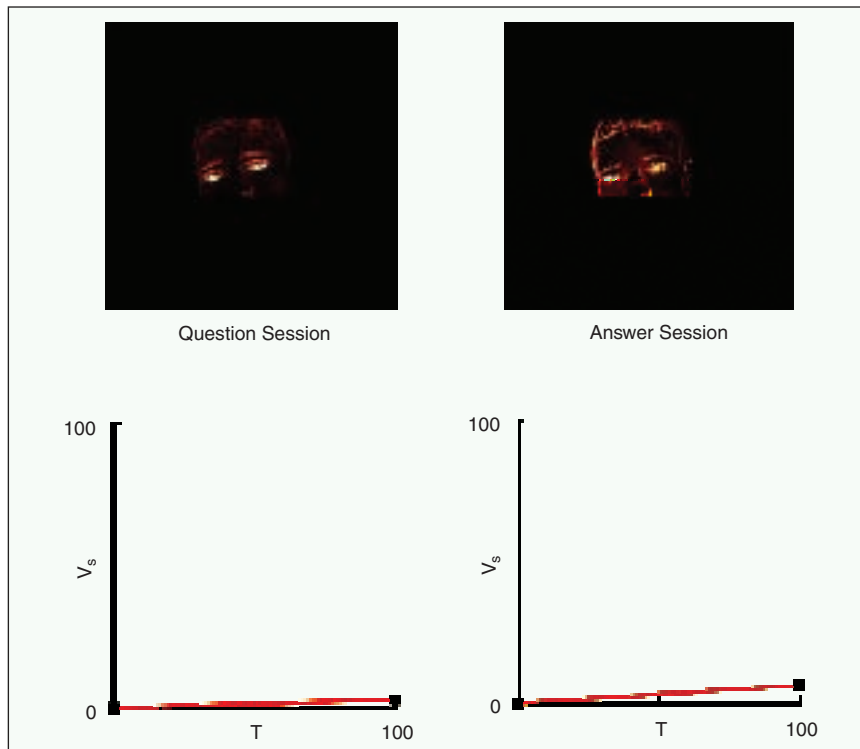
### Pattern Classification

We have found through visual observation that only the "eye" signals in the Zone Comparison Test carry significant discriminating power. This observation was consistent with our previous laboratory findings [1], [2] about the importance of periorbital blood flow rate in anxious states. One important restriction was that the subjects should not wear eyeglasses during the examination. Glass is opaque in the mid- and far-infrared and therefore would clutter the periorbital thermal signature [7]. This restriction was very easy to enforce in the controlled environment associated with polygraph testing.

The "forehead" signals did not appear as discriminating. We also identified some practical problems associated with the monitoring of forehead areas. A com-



5. "Eye" curves for all subjects for Question 10 (Q10) in run 1. During question posing (up to frame 150) there is little differentiation in the slope of the curves. During answer giving (from frame 151 up to frame 300) there is significant differentiation in the slope of the curves.



6. Snapshots of facial blood flow rate during the question and answer sessions for Question 10 (Q10) of the Zone Comparison Test. The snapshots depict Subject 9 (S9), who was programmed nondeceptive. Below the snapshots appear the normalized lines characterizing the slopes of the average periorbital blood flow rate  $V_S$  per time  $T$ . The slopes appear to be very moderate during both the question and the answer sessions.

mon problem is exemplified in Figure 4 where hair bangs fall off the forehead of the subject and clutter the thermal signature of the underlying skin.

A careful visual observation of the “eye” signals reveals that there are two stages of physiological response in a question-answer session for a subject. Initially, during the posing of the question, the “eye” curves ascend moderately for all subjects. Then, as the subjects respond to the question there seems to be a differentiation: the “eye” curves of some subjects continue to ascend moderately while the “eye” curves of others feature a much steeper ascend (see Figure 5). According to our physiological hypothesis, increased blood flow circulation around the eyes is associated with anxious states. Therefore, steep “eye” curves during the answer session are indicative of a deceptive answer.

The question stage lasts the first 150 frames while the answer stage starts from about the frame 151 and lasts all the way to the end of the individual thermal clip (usually up to frame 300). The “eye” curves appear to start from the origin of the coordinate system because we zero the initial conditions for the solution of the differential equation (5). In other words, our measurements should be interpreted in a comparative setting, since only a “dead subject” has zero initial blood flow rate. This comparative measurement setting is perfectly fine for polygraph testing purposes since we are only interested in the relative rate of ascend for the “eye” curves.

A more detailed visual representation of facial blood flow rate patterns and the corresponding “eye” curve slopes is given in Figures 6 and 7. Figure 6 shows Subject 9 (S9), who was programmed nondeceptive by the polygraph psychologists, while Figure 7 shows Subject 29 (S29), who was programmed deceptive. The disparity of the “eye” slopes in the corresponding answer sessions is obvious.

We use as a feature for the classifier the product of the slopes of the “eye” curves in the corresponding question and answer sessions. Ideally, the slope products should form a bimodal distribution, one for the nondeceptive subjects and one for the deceptive subjects. We test this hypothesis by feeding the slope products into a thresholding algorithm. Then, we use the threshold to make binary decisions. If the slope product of an “eye” curve is smaller than the threshold, then

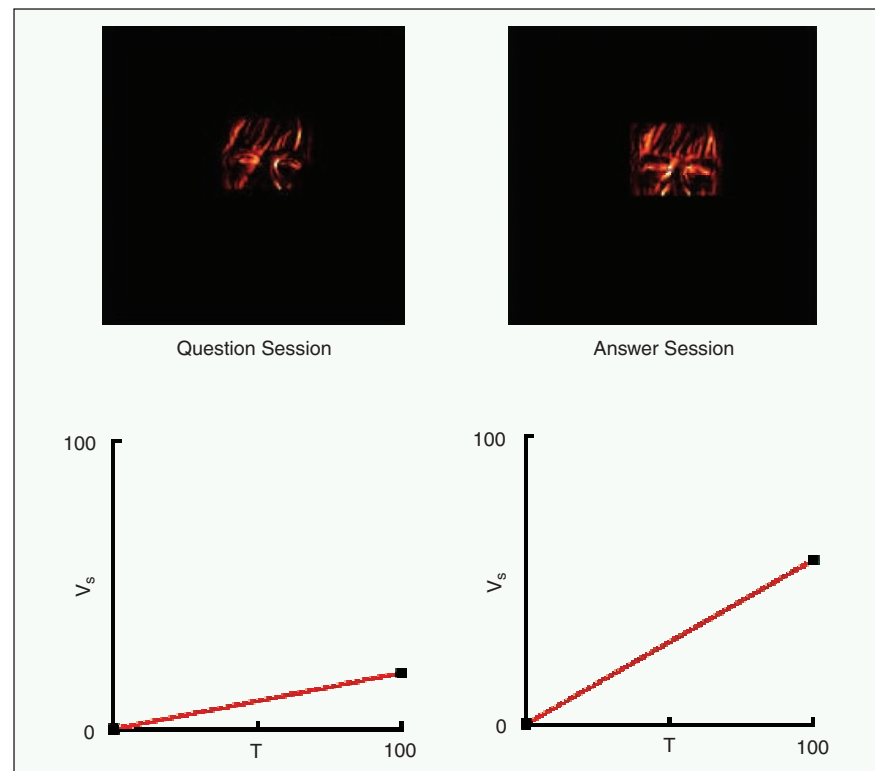
**According to our  
physiological  
hypothesis, increased  
blood flow circulation  
around the eyes is  
associated with  
anxious states.**

we classify the answer as nondeceptive. If the slope product of an “eye” curve is larger than the threshold, then we classify the answer as deceptive.

We have chosen to apply the thresholding algorithm by Otsu [7] because of its excellent performance in bimodal distributions. It involves a nonparametric and unsupervised method of threshold selection. An optimal threshold is selected in order to maximize the separability of the resultant classes. The algorithm utilizes only the zeroth- and the first-order cumulative moments of the histogram. The classification results are presented and discussed in the following section.

**Experimental Results**

We examined a set of 32 polygraphy subjects. Data from only 22 of those were deemed of legitimate use. We lost data from ten subjects due to sizeable human and machine errors (“contamination”). From the 22 admissible subjects we further excluded four subjects because their polygraph examination took place immediately after lunch. We anticipate that the metabolic heat component immediately after a hearty meal is significant and the heat transfer model we currently use cannot handle this case.



**7. Snapshots of facial blood flow rate during the question and answer sessions for Question 10 (Q10) of the Zone Comparison Test. The snapshots depict Subject 29 (S29), who was programmed deceptive. Below the snapshots appear the normalized lines characterizing the slopes of the average periorbital blood flow rate  $V_s$  per time  $T$ . The slope of the answer session appears to be quite steep.**

For all of the 18 down-selected subjects, we were able to score through thermal image analysis only Question 10 (Q10) of the Zone Comparison Test. For the remaining questions we were missing thermal recordings for one to two subjects. These glitches in the completeness of our data set were the result of stringent real-time recording requirements and the inadequacy of our current man-machine interface. Fortunately, Question 10 (Q10) is one of the most important questions in the determination of guilt or innocence for a subject, and therefore, the validity of our results remains quite relevant.

Table 3 shows the classification results by the thermal image analysis system vis-à-vis those by traditional polygraph analysis. By observing the color code for the table, one finds that our thermal image

analysis method achieves a correct classification rate of  $CCR = 84\%$  while the traditional analysis method achieves  $CCR = 78\%$ . The feature for thermal classification is the product of slopes of the “eye” curve during the question and answer sessions for Question 10 (Q10) of the Zone Comparison Test. The slopes are expressed as the angle of the curve (in degrees) at frames 0 and 151 respectively. The list of slope products is ordered from the minimum to the maximum value. Small slope product values correspond to nondeceptive answers while large slope values correspond to deceptive answers. The pink-colored cells depict deceptive subjects that were classified correctly. The ground-truth information was provided from the polygraph psychologists who programmed the subjects. In step

with our physiological hypothesis, all the deceptive cases are clustered at the bottom of the ordered list.

Although the clustering appears to be ideal, from the classification point of view the question is how do we know where to draw the threshold. By applying the thresholding algorithm by Otsu [7] as explained in the previous section, we get a threshold value  $th = 67^\circ$ . Then we use this value to make binary classification decisions on the slope product list of Table 3.

The reader may gain a better understanding of our experimental data by looking at Figure 8. Figure 8 depicts the “eye” slope products from the most nondeceptive to the most deceptive subject in a radar graph form. All the slope products that are external to the second in-

**Table 3. Ordered list of “eye” slope products for Question 10 (Q10) from the Zone Comparison Test. The slopes are expressed as angles in degrees. Also, the table features the scoring of the same question by the traditional method using invasive measurements. The traditional scale ranges from -5 to +5, where non-negative values denote nondeceptive answers, while negative values indicate deceptive answers.**

Thermal Scoring		Traditional Scoring	
Subject	Slope Product	Subject	Deceptive Index
Subject 9	10.2	Subject 9	-2
Subject 8	17.0	Subject 8	2
Subject 17	18.5	Subject 17	2
Subject 5	18.5	Subject 5	1
Subject 12	28.6	Subject 12	2
Subject 14	30.2	Subject 14	-2
Subject 15	33.9	Subject 15	0
Subject 18	34.6	Subject 18	2
Subject 23	37.1	Subject 23	-1
Subject 25	45.9	Subject 25	3
Subject 10	48.7	Subject 10	0
Subject 21	67.1	Subject 21	-1
Subject 19	94.5	Subject 19	-3
Subject 13	96.8	Subject 13	4
Subject 20	114.0	Subject 20	-2
Subject 3	115.5	Subject 3	-2
Subject 6	216.7	Subject 6	0
Subject 29	326.7	Subject 29	-3
Color Code		Correct Non-Deception Detection	
		Correct Deception Detection	
		False Alarm	
		Missed Detection	

ner circle are classified as deceptive by our method.

An interesting qualitative verification as to the accuracy with which the heat transfer modeling extracts blood flow rate is given in Figure 9. The figure depicts the raw thermal snapshot of a subject's wrist featuring a major vein that runs across. Next to it is depicted the blood flow rate visualization image as it is computed by (5).

### Conclusion

We have designed, developed, and tested a very promising thermal image analysis method for polygraph testing. The method achieved a correct classification rate of  $CCR = 84\%$  on the test population to our avail. This method, once refined, can serve as an additional channel for increasing the reliability and accuracy of traditional polygraph examination.

We extract subtle facial temperature fluctuation patterns through nonlinear heat transfer modeling proposed in [5] and [6]. The modeling transforms raw thermal data to blood flow rate information. Then, we use the slope of the average periorbital blood flow rate as the feature of a binary classification scheme. The results come to support our previous laboratory findings about the importance of periorbital blood flow in anxious states.

In our immediate future plans we contemplate the following steps for enhancing our initial thermal polygraphy method:

- 1) Improve the current heat transfer model by accounting for the metabolic heat factor. Then, the performance of the method will become independent of the time elapsed since the subject's last significant meal.

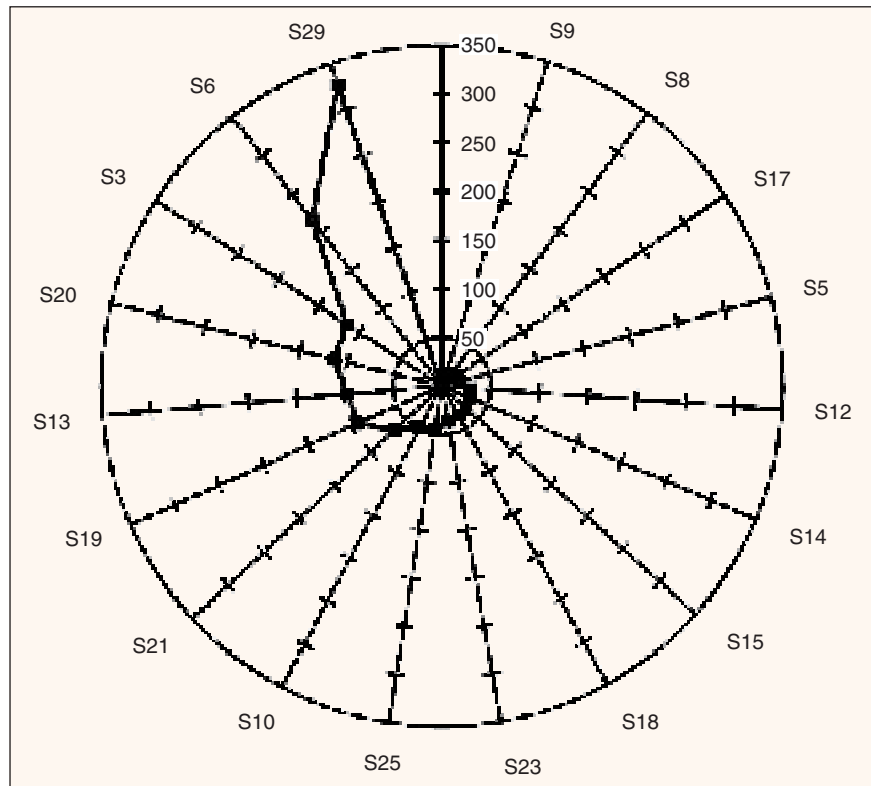
- 2) Develop an algorithm that will track the human head as it moves around during the length of the polygraph testing. This is of fundamental importance for the accurate solution of the differential heat transfer equation that operates pixel-wise and across frames. Currently, we solve this equation assuming a completely stationary subject for short periods of time. This is a practical but not extremely accurate assumption. Some of the most agitated subjects move noticeably through each question-answer session. For the time being, we exclude these subjects from consideration by reducing even further the proportion of usable data.

- 3) Corroborate through medical research the parameter values in the heat transfer equation. Currently, we drop

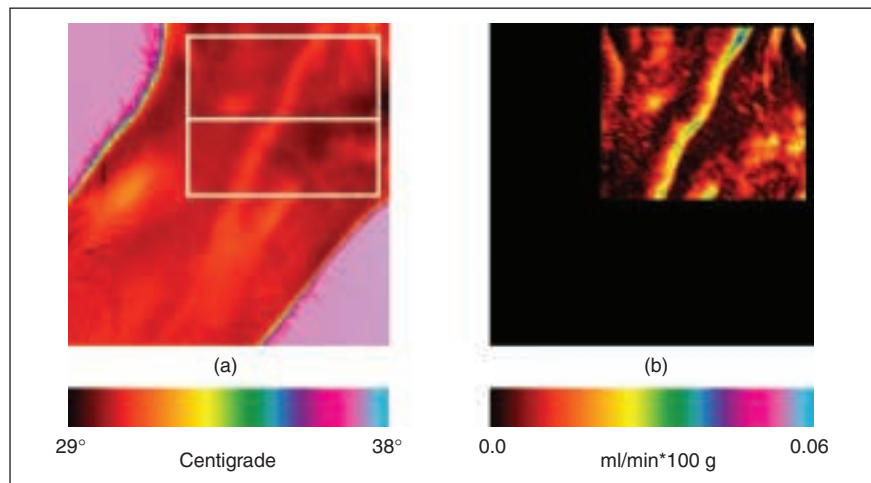
these parameters and compute the blood flow rate with accuracy up to a multiplicative factor.

- 4) Assuming that we have the face tracker in place, we can develop a network of fiducial points where we will monitor the blood flow rate across the face over time. In this manner we will start making true use of the 2-D nature of our informa-

tion. Please note that we currently compute the average blood flow rate in the periorbital area and in essence we fall back to 1-D (signal) information. Averaging the blood flow rate over a substantial facial area is more tolerant to registration errors and is the only practical alternative in the absence of a facial tracker.



8. The "eye" slope values depicted in radar graph form. All the slope values outside the second inner circle belong to subjects programmed deceptive. This is another visual confirmation of the bimodality of the slope feature.

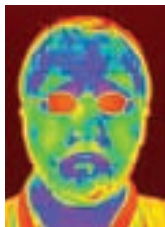


9. (a) Raw thermal image of a human wrist. (b) The corresponding blood flow rate visualization image. The color bars at the bottom index colors to values from the minimum to the maximum of the respective ranges.

5) Perform further experiments to increase our training and testing base. This will allow us to validate our current algorithmic apparatus against a more substantial subject database. In this context, we plan on developing a more sophisticated man-machine interface that will facilitate real-time capturing and labeling of thermal video data. It is our bitter experience that the lack of such an interface may result in the loss or compromise of almost half of the real-time experimental data.

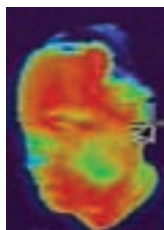
### Acknowledgments

Most of the research work described in the article was carried out at Honeywell Laboratories and some small part at the University of Houston. Our research was supported by grant #DABT60-00-1-1003. We would like to thank Dr. Andrew Ryan, chief of research at the DoD Polygraph Institute, for his generous support. We would also like to acknowledge the valuable help of Dr. Dean Pollina, research psychologist at the DoD Polygraph Institute. Finally, we would like to thank Dr. Peter Symosek, Dr. Vassilios Morellas, and Pete Roeber for their substantial support during the software implementation phase.



*Ioannis Pavlidis* (thermal image shown) holds a Ph.D. and an M.S. degrees in computer science from the University of Minnesota, an M.S. degree in robotics from the Imperial College of the University of London, and a B.S. degree in electrical engineering from the Democritus University in Greece. He joined Honeywell Laboratories immedi-

ately upon his graduation in January 1997. His expertise is in the areas of computer vision beyond the visible spectrum and pattern recognition of highly variable patterns. Dr. Pavlidis published extensively in these areas in major journals and refereed conference proceedings over the past several years. He is the co-chair of the IEEE series of Workshops in Computer Vision Beyond the Visible Spectrum and serves as a program committee member in several other major conferences. Dr. Pavlidis is a Fulbright Fellow, a Senior Member of IEEE, and a member of ACM. Dr. Pavlidis has joined the faculty of the Computer Science Department at the University of Houston as of September 2002.



*James Levine* (thermal image shown) holds a Ph.D. in medicine, an M.B.B.S. in clinical nutrition and medicine, and a B.Sc. in clinical nutrition, all from the Royal Free Hospital School of Medicine in London. Dr. Levine is a world authority on measurements of metabolic rate and energy expenditure. He is also technically adept and experienced with instrument design and validation. His Ph.D. included writing development and validation of a novel electronic device for measuring local heat loss and writing of a novel software suite. Dr. Levine is widely accomplished in human research having completed numerous high-profile projects all focused on how metabolic rate (synonymous with heat loss) is fine-tuned. Dr. Levine currently runs a staffed laboratory dedicated to high precision measurements of metabolic rate. He sits on the General Clinic Research Center Committee at the Mayo Clinic and is a

co-director of the Minnesota Obesity Center and an invited Professor to Endocrinology 2000 and the American College of Nutrition. Dr. Levine is a member of the North America Society for the Study of Obesity, the American Medical Association, and the Endocrine Society.

**Address for Correspondence:** Ioannis Pavlidis, University of Houston, Houston, Texas, USA. E-mail: pavlidis@cs.uh.edu.

### References

- [1] I. Pavlidis, J. Levine, and P. Baukol, "Thermal imaging for anxiety detection," in *Proc. 2000 IEEE Workshop on Computer Vision Beyond the Visible Spectrum: Methods and Applications*, Hilton Head Island, SC, June 16, 2000, pp. 104-109.
- [2] J. Levine, I. Pavlidis, and M. Cooper, "The face of fear," *The Lancet*, vol. 357, no. 9270, June 2001.
- [3] J.A. Matte, *Forensic Psychophysiology Using the Polygraph - Scientific Truth Verification - Lie Detection*. Williamsville, NY: J.A.M. Publications, 1996.
- [4] C. Holden, "Panel seeks truth in lie detector debate," *Science*, vol. 291, no. 9, p. 967, 2001.
- [5] M. Iwatani, "An estimation method of skin blood flow rate using heat flow analysis," *Jap. J. Medical Electron. Biologic. Eng.*, vol. 20, no. 3, pp. 249-255, 1982.
- [6] I. Fujimasa, T. Chinzei, and I. Saito, "Converting far-infrared image information to other physiological data," *IEEE Eng. Med. Biol. Mag.*, vol. 19, no. 3, pp. 71-75, 2000.
- [7] I. Pavlidis, P. Symosek, B. Fritz, M. Bazakos, and N.P. Papanikolopoulos, "Automatic detection of vehicle occupants - The imaging problem and its solution," *Machine Vision Applicat.*, vol. 11, no. 6, pp. 313-320, 2000.
- [8] N. Otsu, "A threshold selection method from gray-level histograms," *IEEE Trans. Systems, Man, Cybernetics*, vol. 9, no. 1, pp. 62-65, 1979.